[RADIOCARBON, VOL. 36, NO. 3, 1994, P. 327–343]

Radiocarbon

1994

ON THE ^{14}C AND ^{39}Ar DISTRIBUTION IN THE CENTRAL ARCTIC OCEAN: IMPLICATIONS FOR DEEP WATER FORMATION[1]

PETER SCHLOSSER,[2,3] BERND KROMER,[4] GOTE ÖSTLUND,[5] BRENDA EKWURZEL,[2,3] GERHARD BÖNISCH,[2] H. H. LOOSLI[6] and ROLAND PURTSCHERT[6]

ABSTRACT. We present $\Delta^{14}C$ and ^{39}Ar data collected in the Nansen, Amundsen and Makarov basins during two expeditions to the central Arctic Ocean (RV *Polarstern* cruises ARK IV/3, 1987 and ARK VIII/3, 1991). The data are used, together with published $\Delta^{14}C$ values, to describe the distribution of $\Delta^{14}C$ in all major basins of the Arctic Ocean (Nansen, Amundsen, Makarov and Canada Basins), as well as the ^{39}Ar distribution in the Nansen Basin and the deep waters of the Amundsen and Makarov Basins. From the combined $\Delta^{14}C$ and ^{39}Ar distributions, we derive information on the mean "isolation ages" of the deep and bottom waters of the Arctic Ocean. The data point toward mean ages of the bottom waters in the Eurasian Basin (Nansen and Amundsen Basins) of *ca.* 250–300 yr. The deep waters of the Amundsen Basin show slightly higher ^{3}H concentrations than those in the Nansen Basin, indicating the addition of a higher fraction of water that has been at the sea surface during the past few decades. Correction for the bomb ^{14}C added to the deep waters along with bomb ^{3}H yields isolation ages for the bulk of the deep and bottom waters of the Amundsen Basin similar to those estimated for the Nansen Basin. This finding agrees well with the ^{39}Ar data. Deep and bottom waters in the Canadian Basin (Makarov and Canada Basins) are very homogeneous, with an isolation age of *ca.* 450 yr. $\Delta^{14}C$ and ^{39}Ar data and a simple inverse model treating the Canadian Basin Deep Water (CBDW) as one well-mixed reservoir renewed by a mixture of Atlantic Water (29%), Eurasian Basin Deep Water (69%) and brine-enriched shelf water (2%) yield a mean residence time of CBDW of *ca.* 300 yr.

INTRODUCTION

Measurements of the radioactive isotope of carbon, ^{14}C, have frequently been used for determining circulation patterns and mean residence times of the deep and bottom waters in the world ocean (see, *e.g.*, Broecker *et al.* 1960, 1985; Münnich and Roether 1967; Stuiver, Quay and Östlund 1983). The application of ^{14}C in oceanographic studies is based on the conversion of the activity gradient between surface waters and deep waters into a mean *age* of the deep waters (see, *e.g.*, Broecker *et al.* 1991). During the past decades, a fairly good ^{14}C data set has been assembled for most major ocean basins. However, due to the limited access to ice-covered regions, the database for the Arctic Ocean has been comparably sparse for a long time, during which the only platforms for collection of ^{14}C data have been ice camps (see, *e.g.*, Östlund, Top and Lee 1982; Östlund, Possnert and Swift 1987). Only since the mid-1980s have we been able to collect ^{14}C data with good spatial resolution in the Arctic Ocean (for first results, see Schlosser *et al.* 1990, 1995).

The purpose of this contribution is to combine new ^{14}C data collected during two cruises of the German research icebreaker *Polarstern* to the central Arctic Ocean with those available in the literature to describe the ^{14}C distribution in the central Arctic Ocean. In addition, we present an ^{39}Ar data set

[1]This paper was presented at the 15th international Radiocarbon Conference, 15–19 August 1994, Glasgow, Scotland.

[2]Lamont-Doherty Earth Observatory of Columbia University, Palisades, New York 10964 USA
[3]Department of Geological Sciences of Columbia University, Palisades, New York 10964 USA
[4]Institut für Umweltphysik der Universität Heidelberg, Im Neuenheimer Feld 366, D-69120 Heidelberg, Germany
[5]Rosenstiel School of Marine and Atmospheric Science, University of Miami, Rickenbacker Causeway, Miami, Florida 33149 USA
[6]Physikalisches Institut der Universität Bern, Sidlerstrasse 5, CH-3012 Bern, Switzerland

from the Nansen, Amundsen and Makarov Basins, which we use to strengthen the conclusions drawn from the $\Delta^{14}C$ data; we also derive mean ages of the deep and bottom waters in the Arctic Ocean. Due to the limited data sets, some of our conclusions are preliminary. The final evaluation of the data, in combination with other steady-state and transient tracers, is beyond the scope of this paper, and will be presented in a follow-up study.

Description of the Data Set

The data set used in this paper consists of three parts: 1) A ^{14}C section collected during the 1987 crossing of the Nansen Basin by RV *Polarstern* (Fig. 1). These data, as well as the methods used for collection and measurement of large volume (LV) ^{14}C, accelerator mass spectrometry (AMS) ^{14}C and ^{39}Ar samples, have been described previously (Schlosser *et al.* 1990, 1995); 2) ^{14}C profiles and ^{39}Ar samples collected in the Nansen, Amundsen and Makarov Basins during the ARCTIC 91 expedition on board RV *Polarstern* (Fig. 1). The ^{14}C data from this cruise are exclusively high-precision

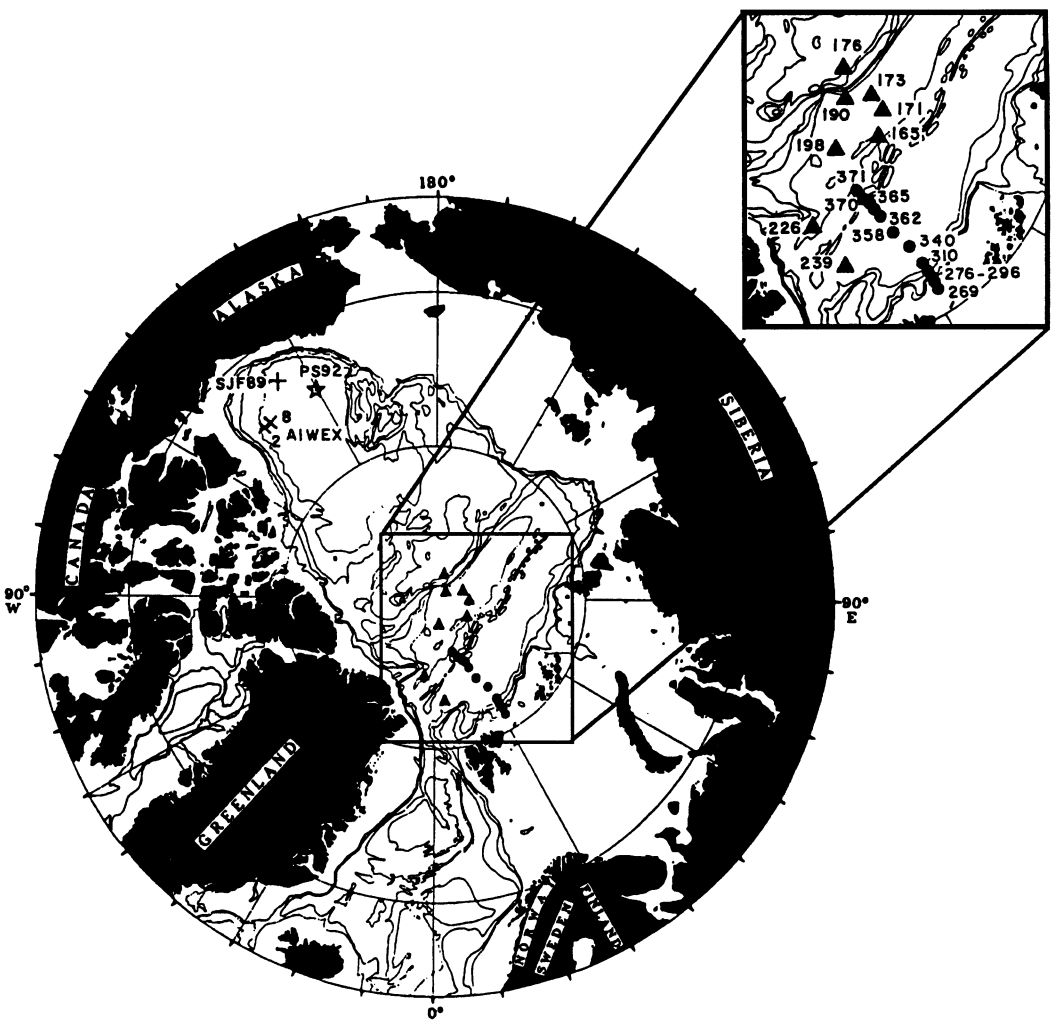

Fig. 1. Geographical position of the ^{14}C and ^{3}H stations in the Amundsen, Nansen, Makarov and Canada Basins

LV measurements performed in the ^{14}C laboratory of the University of Heidelberg. Sample collection and measurement procedures are identical to those used for the LV samples collected during the 1987 expedition and are described by Schlosser *et al.* (1995); 3) Three published ^{14}C profiles from the Canadian Basin (Makarov Basin: one profile (Östlund, Possnert and Swift 1987); Canada Basin: two profiles (Macdonald and Carmack 1991; Jones *et al.* 1994)). The ^{14}C data from the Makarov Basin are from the 1979 Lomonosov Ridge Experiment (LOREX) ice camp; LV measurements were made at the University of Miami. The data published by Macdonald and Carmack (1991) and by Jones *et al.* (1994) are AMS data collected during the 1989 CCGS *Sir John Franklin* cruise (SJF) and the 1992 USCG *Polar Star* cruise (PS 92). They were measured at the IsoTrace AMS laboratory of the University of Toronto and at the Woods Hole Oceanographic Institution National Oceanographic AMS facility, respectively. Figure 1 summarizes geographical positions of all stations.

The ^{3}H measurements used to indicate the penetration of bomb ^{14}C into the water column were measured at the University of Heidelberg (ARK IV) and at the University of Miami (ARK VIII and Canada Basin Station SJF; Fig. 1). It is evident from Figure 1 that presently we have the best coverage for the Nansen and Amundsen Basins, whereas the database for the Canadian Basin is still fairly sparse. However, the new data from the ARCTIC 91 expedition presented below allow us, for the first time, to compare ^{14}C data from all major deep basins of the Arctic Ocean. Additionally, it provides the first ^{39}Ar data from the Canadian Basin.

Hydrographic Background

To provide background for the discussion of the ^{14}C data, we briefly summarize the main hydrographic features of the Arctic Ocean, following the work of Aagaard, Swift and Carmack (1985). We use their section of potential temperature, salinity and potential density across the Iceland-Greenland-Norwegian Seas and the Arctic Ocean (for geographic position of the stations in this section, see Fig. 2). The focus of the description will be on the Arctic Ocean portion of the section.

The hydrographic section across the Arctic Ocean (north of Fram Strait) is dominated by three water masses: 1) upper waters; 2) Atlantic-derived water; and 3) deep water. The upper waters are divided into the Polar mixed layer (PML; 30–50 m deep) and the halocline (*ca.* 30–50 to *ca.* 200 m deep; Fig. 3). The PML is cold (temperatures close to the freezing point) and fresh due to the impact of Arctic river runoff. The halocline consists of water advected into the interior basins from the Arctic shelves where it is preconditioned by sea-ice formation during winter (see, *e.g.*, Aagaard, Coachman and Carmack 1981). Jones and Anderson (1986) used nutrient measurements in addition to T/S considerations to distinguish between upper halocline waters (UHW: $S \approx 33.1$) originating in the Bering and Chukchi Seas, and lower halocline waters (LHW: $S \approx 34.2$) produced most likely in the Barents and Kara Seas.

The Atlantic-derived water underlies the halocline waters. It is defined as the layer with temperatures above 0°C, and is typically found at depths ranging from *ca.* 200–800 m. The deep waters below the Atlantic derived waters are relatively low in potential temperature (≈ -0.95°C in the Eurasian Basin and ≈ -0.5°C in the Canadian Basin) and high in salinity (≈ 34.945 at 3000 m depth in the Eurasian Basin and ≈ 34.955 at the same depth in the Canadian Basin). Smethie *et al.* (1988) divide the deep waters of the Nansen Basin into Eurasian Basin Deep Water (EBDW: $32.921 < S < 34.927$; -0.96°C $< \Theta < -0.70$°C) and Eurasian Basin Bottom Water (EBBW: $34.930 < S < 34.945$; -0.95°C $< \Theta < -0.94$°C). The reason for the freshness of the Eurasian Basin deep waters is probably linked to exchange of deep waters with the Norwegian and Greenland Seas. The density gradient in the Arctic Ocean water column is strongest in the halocline and weakest in the deep waters of the Canadian Basin (see σ_3 section in Fig. 3).

Fig. 2. Geographical position of the stations used to construct the section plotted in Fig. 3 (from Aagaard *et al.* 1985; © by the American Geophysical Union).

Results

Nansen Basin

The $\Delta^{14}C$ profiles from the 1987 Nansen Basin section are divided into three groups representing the southern, central and northern Nansen Basin, respectively (Fig. 4). Each group of profiles is further divided into a plot displaying the entire water column (Figs. 4A–C) and a plot of the deep waters (depth >1500 m; Figs. 4D–F). The $\Delta^{14}C$ profiles show several characteristic features: 1) The surface water $\Delta^{14}C$ values increase from south (≈ 50–80‰; Figs. 4A–B) to north (≈ 120‰; Fig. 4C). This increase reflects the higher fraction of river runoff in the surface waters of the northern part of the section (Schlosser *et al.* 1994; Bauch, Schlosser and Fairbanks 1995); 2) The average $\Delta^{14}C$ values in the core of the Atlantic-derived layer (maximum in potential temperature located at ≈ 200–300 m

depth) are fairly constant throughout the section (≈ 50‰); Figs 4A–C). The Atlantic-derived layer is eroded toward the north, which is reflected in the fairly thin water layer with $\Delta^{14}C$ values close to 50‰ (Fig. 4C); 3) Between the core of the Atlantic-derived water marked by the temperature maximum and the deep water (here defined as water below 1500 m depth), the $\Delta^{14}C$ values drop fairly

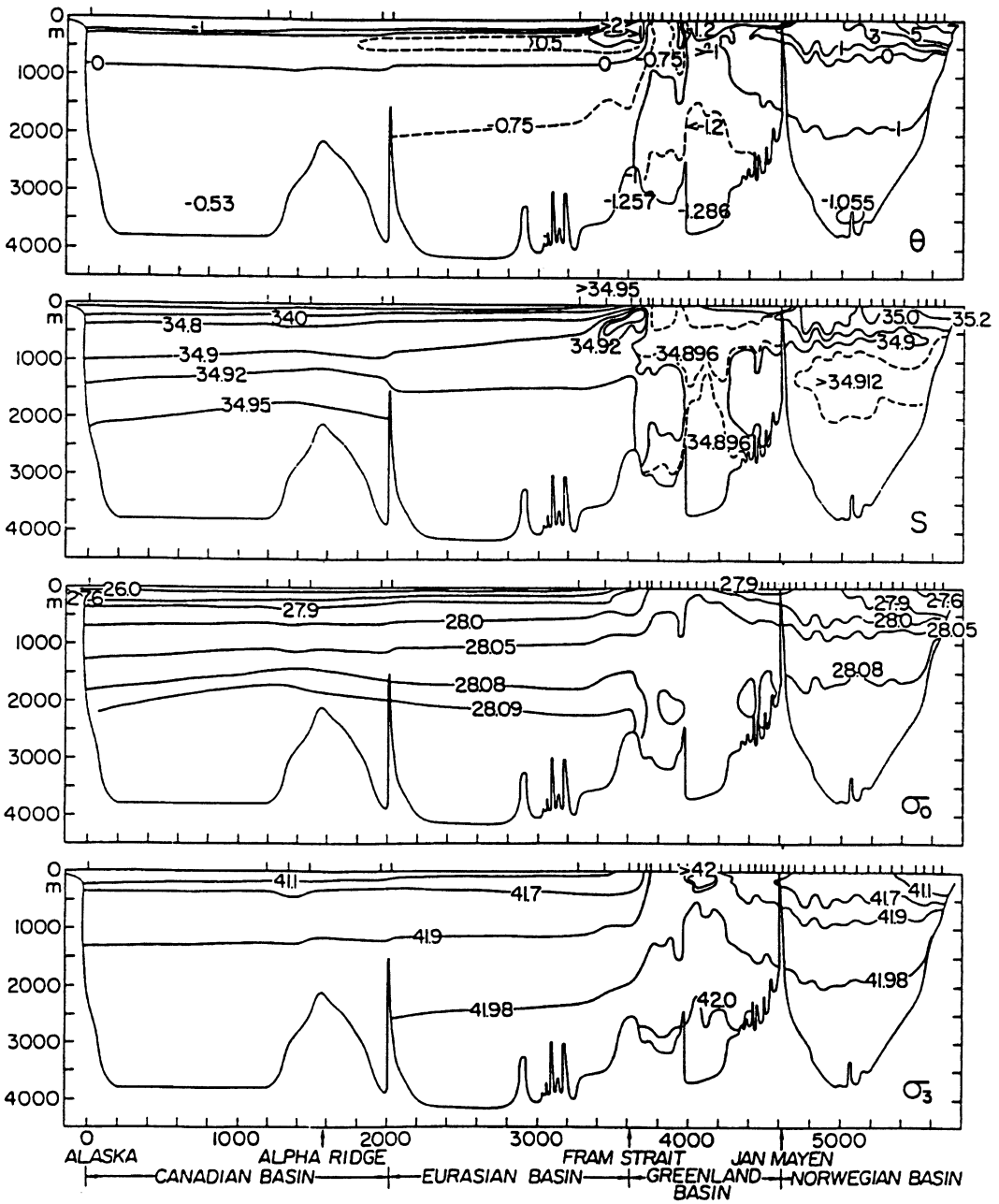

Fig. 3. Section of potential temperature (θ), salinity (S) and density (σ_0 and σ_3) along a section across the Greenland-Iceland-Norwegian Seas (from Aagaard *et al.* 1985; © by the American Geophysical Union).

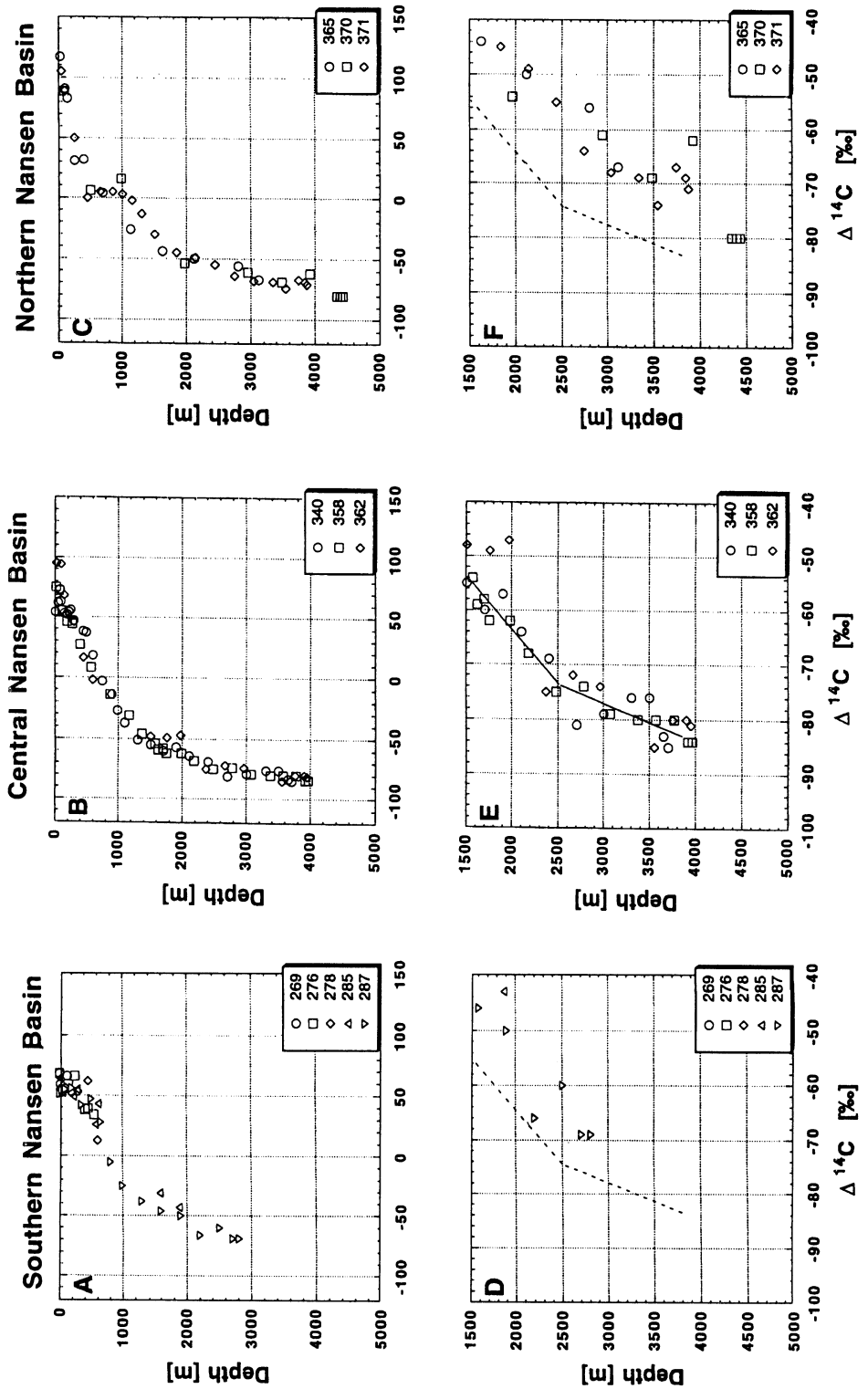

Fig. 4. A. $\Delta^{14}C$ profiles from the Southern; B. Central; C. Northern Nansen Basin (for geographical position of the stations, see Fig. 1); D–F. Deepwater column (≥1500-m depth) shown on an extended scale. - - - = shape of the $\Delta^{14}C$ profile in the Central Nansen Basin.

monotonically to values of *ca.* −50‰ in the southern and central Nansen Basin (Figs. 4A, B), whereas a clear inflection of water with somewhat higher $\Delta^{14}C$ values in the northern Nansen Basin centers at *ca.* 1000 m (Fig. 4C); 4) The $\Delta^{14}C$ profiles in the deep and bottom waters show a distinct break at *ca.* 2500 m in the central Nansen Basin (Fig. 4E). This depth coincides with the sill depth of Fram Strait. The break is not observed in the southern and northern Nansen Basin (Figs. 4D, F). The lowest $\Delta^{14}C$ values of the deep and bottom waters (≈ −80 to −85‰) are observed in the central Nansen Basin (Fig. 4E), whereas $\Delta^{14}C$ values in the bottom waters of the southern and northern parts of the section (Figs. 4D, F) are slightly higher (≈ −70‰). However, the bottom waters at Station 370 located in the trough of the Gakkel Ridge have $\Delta^{14}C$ values close to those in the central Nansen Basin.

The ^{3}H profiles (Fig. 5) from corresponding stations show features similar to those observed in the $\Delta^{14}C$ profiles. They are used as indicators of the penetration of bomb ^{14}C into the water column. The concentrations of ^{3}H in the bottom waters are higher in the northern and southern Nansen Basin (≈ 0.3 TU; Figs. 5D, F; 1 TU means a ^{3}H-to-hydrogen ratio of 10^{-18}) than in the central Nansen Basin (≈ 0.05 TU; Fig. 5E).

The ^{39}Ar data collected in the Nansen Basin show a constant decrease between surface waters (92% modern at Station 269) and bottom waters (46% modern at Station 358; Fig. 10). Resolution is not sufficient in the ^{39}Ar distribution to resolve potential lateral gradients in the Nansen Basin.

Amundsen Basin

The $\Delta^{14}C$ profiles available from the Amundsen Basin (Fig. 6) have the closest similarity to those of the northern Nansen Basin: 1) They show basically the same surface $\Delta^{14}C$ values of ≈ 120‰; 2) $\Delta^{14}C$ values are ≈ 50‰ in the Atlantic layer at *ca.* 250–300 m depth; 3) an inflection of waters with relatively high $\Delta^{14}C$ values is observed at *ca.* 1000 m depth (most pronounced at Station 190, located closest to the Lomonosov Ridge); and 4) $\Delta^{14}C$ values in the bottom waters are significantly higher (5–7‰) than those observed in the central Nansen Basin (Fig. 6B). Station 239 included in Figure 6 is actually located in the southern Nansen Basin just north of Fram Strait (Fig. 1). The $\Delta^{14}C$ values of this station are close to values observed in the deep central Nansen Basin. The $\Delta^{14}C$ profiles of the Amundsen Basin show a distinct break at a depth of *ca.* 3000 m. This feature is very similar to that observed in the central Nansen Basin, although at a slightly lower depth (3000 m compared to ≈ 2500 m; Fig. 6B). Only one full ^{3}H profile is available from the Amundsen Basin (Sta. 173; Fig. 7). It shows penetration of significant levels of bomb ^{3}H into the bottom waters (≈ 0.2 TU).

^{39}Ar concentrations in the deep Amundsen Basin range from 71% modern (Station 173; 1900-m depth) to 55% modern (Station 173; 4300-m depth; Fig. 10).

Makarov Basin

The only high-resolution $\Delta^{14}C$ profile available from the Makarov Basin is Station 176, occupied during the ARCTIC 91 expedition (Figs. 6A and 8A). In the upper 200 m, the structure is similar to that observed in the Nansen and Amundsen Basins. Below this depth, the $\Delta^{14}C$ values in the Makarov Basin are much lower throughout the water column than those in the Eurasian Basin (Nansen and Amundsen Basins). Below 2000 m depth, the $\Delta^{14}C$ values of the deep waters in the Makarov Basin are constant within the analytical precision of the ^{14}C measurement with a mean value of (−104 ± 3)‰. This value is in excellent agreement with the $\Delta^{14}C$ value of −104‰ obtained by from the 1979 LOREX ice camp at 2500 m depth (Östlund, Possnert and Swift 1987). The ^{3}H

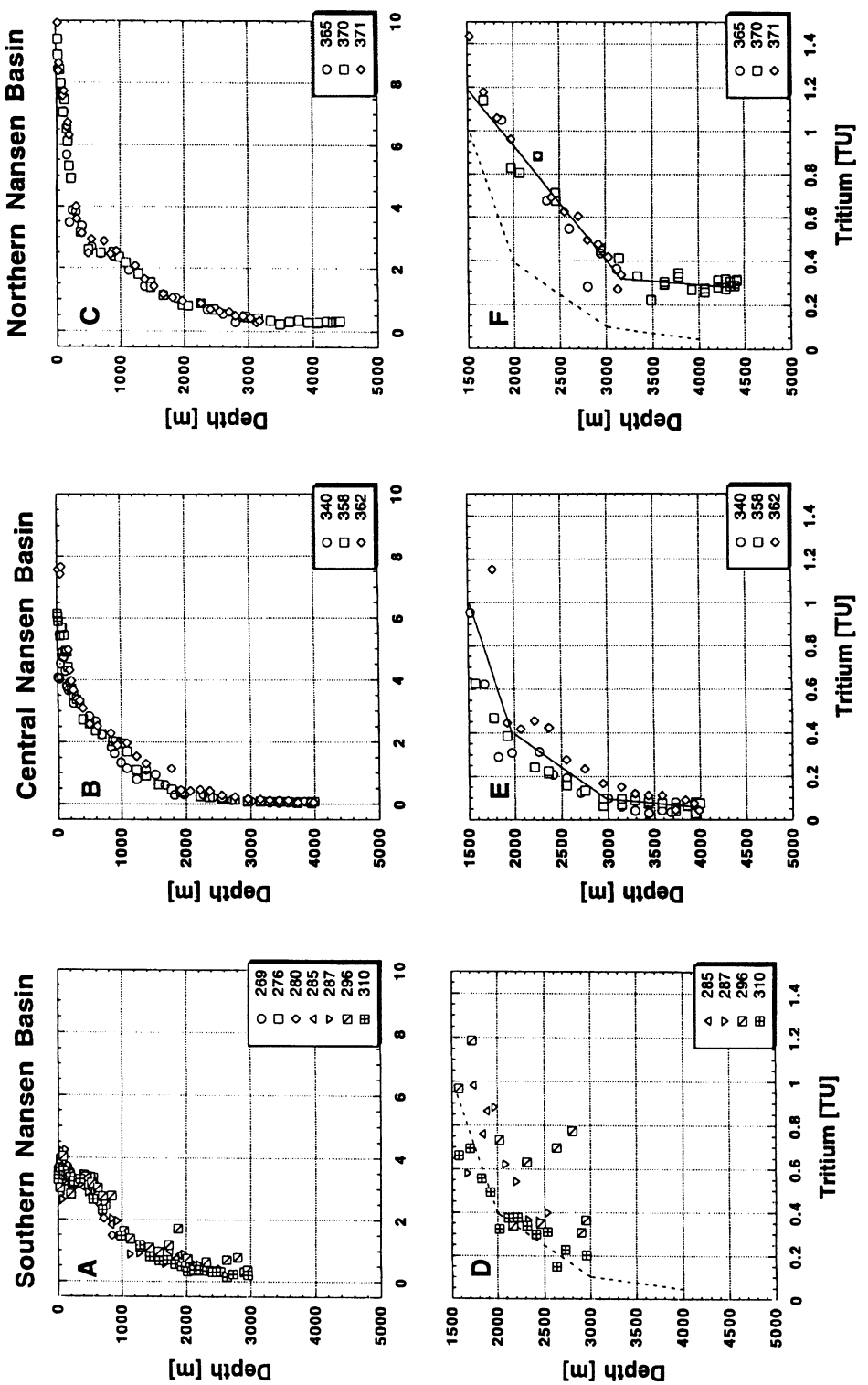

Fig. 5. ^{3}H profiles from the Southern (A), Central (B) and Northern (C) Nansen Basin (for geographical position of the stations, see Fig. 1); D–F. Deepwater column (≥1500 m depth) shown on an extended scale. —— in Figs. E and F = a subjective fit of the data; - - - in D and F = shape of the ^{3}H profile in the Central Nansen Basin.

profile from Station 176 (Fig. 7) indicates that no bomb ^{3}H penetrated below *ca.* 2000 m depth in the Makarov Basin.

^{39}Ar data from the deep Makarov Basin (Fig. 10) are close to 43% modern (range: 50 ± 5 to 35 ± 7% modern). These concentrations are the lowest observed in the Arctic Ocean (≈ 24% modern lower than those in the Eurasian Basin).

Canada Basin

The two $\Delta^{14}C$ profiles from the (southern) Canada Basin (Macdonald and Carmack 1991; Jones *et al.* 1994) show significantly lower surface $\Delta^{14}C$ values compared to the Eurasian and Makarov Basins (≈ 25‰ *vs.* ≈ 120‰; Fig. 8A). Below the surface waters, the $\Delta^{14}C$ values in the Atlantic-

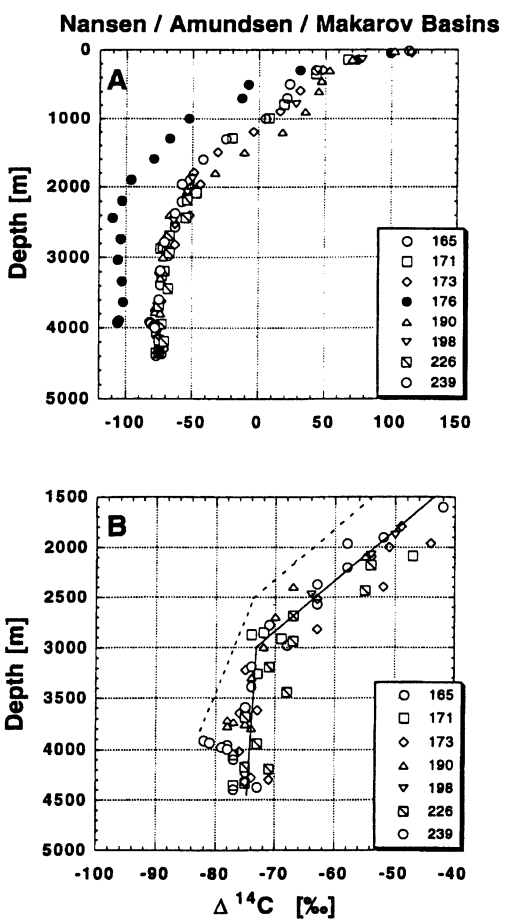

Fig. 6. A. $\Delta^{14}C$ profiles from the Nansen (Sta. 239), Amundsen (Stas. 165, 171, 173, 190, 198, 226) and Makarov (Sta. 176) basins of the Arctic Ocean (for geographical position of the stations, see Fig. 1); B. Deepwater column (≥1500-m depth) shown on an extended scale. —— = subjective fit of the data; - - - = mean $\Delta^{14}C$ profile observed in the Central Nansen Basin.

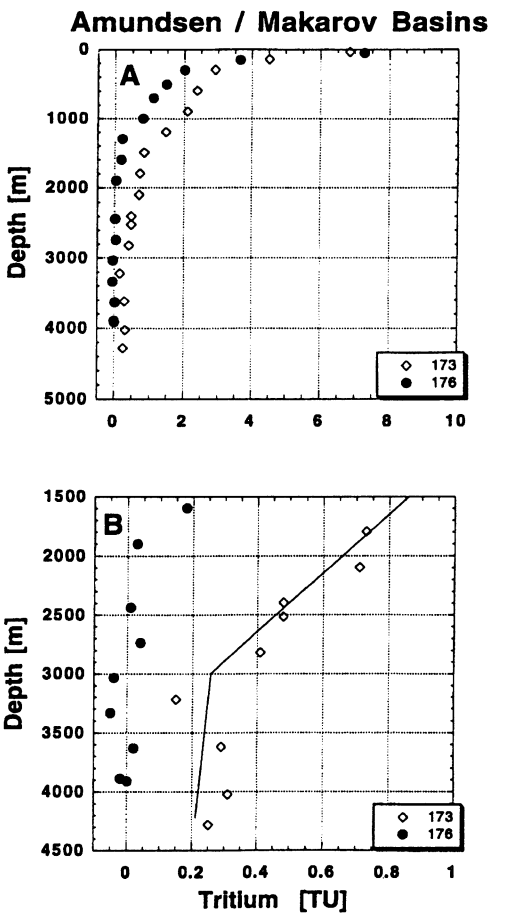

Fig. 7. A. ^{3}H profiles of two stations representative for the Amundsen (Sta. 173) and Makarov (Sta. 176) Basins of the Arctic Ocean (for geographical position of the stations, see Fig. 1). B. Deepwater column (≥1500-m depth) is shown on an extended scale.

derived layer are similar to those observed in the other basins of the central Arctic Ocean (≈ 50‰). Below the core of the Atlantic-derived water (≈ 200–300 m depth), the $\Delta^{14}C$ values in the Canada Basin are higher than those in the Makarov Basin. As in the case of the northern Nansen and the Amundsen Basins, an inflection of water with relatively high $\Delta^{14}C$ values seems to center at *ca.* 1000–1500 m depth. Below 2500 m depth, the $\Delta^{14}C$ values are constant throughout the water column with a mean $\Delta^{14}C$ value of *ca.* (−107 ± 5)‰ (Fig. 8B). This value changes to (−105 ± 2)‰, if one value of the SJF profile with an error of ± 18‰ (Macdonald and Carmack 1991) is omitted in the data set used for calculation of the mean value. The mean value for the waters below 2500 m in the Canada Basin is in excellent agreement with that observed in the waters below 2000 m in the Makarov Basin (−104 ± 3)‰ (see above). The few ^{3}H data available from the deep Canada Basin (Fig. 9) are consistent with those of the Makarov Basin, although the scatter around 0 TU is significantly higher in the Canada Basin than in the Makarov Basin.

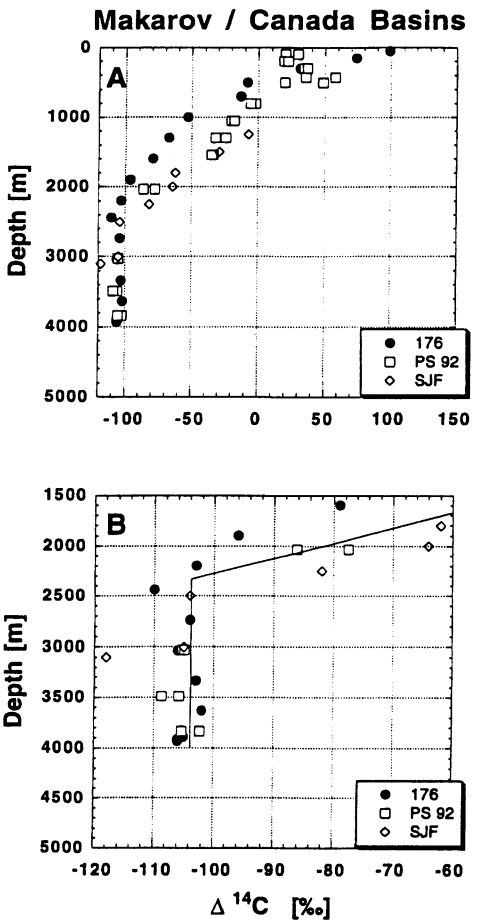

Fig. 8. A. $\Delta^{14}C$ profiles from the Makarov (Sta. 176) and the Canada Basin of the Arctic Ocean (for geographical position of the stations, see Fig. 1). B. The deepwater column (≥1500-m depth) is shown on an extended scale.

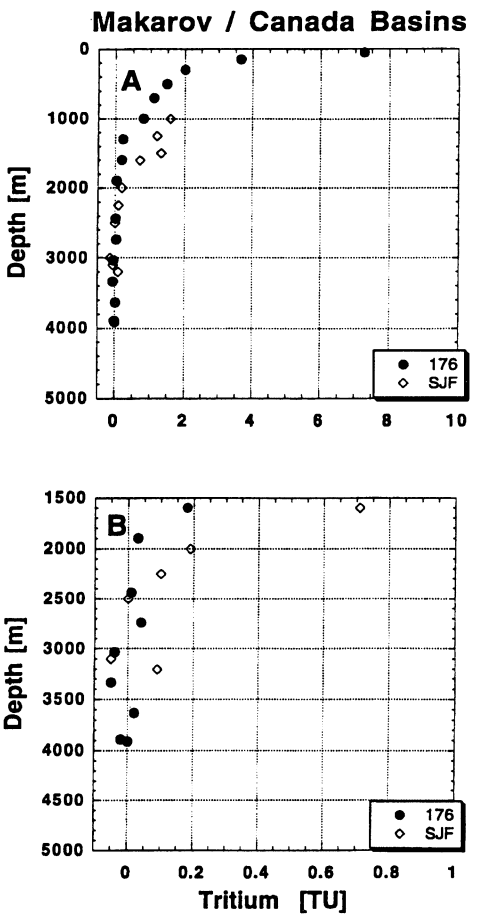

Fig. 9. A. ^{3}H profiles from the Makarov (Sta. 176) and the Canada Basin of the Arctic Ocean. The data from the Canada Basin are from a 1989 cruise of the SJF (Macdonald and Carmack 1991). For geographical position of the stations, see Fig. 1. B. Deepwater column (≥1500-m depth) is shown on an extended scale.

Discussion

Upper Waters

The upper waters are dominated by bomb ^{14}C. According to Östlund, Possnert and Swift (1987), pre-bomb $\Delta^{14}C$ values reached from *ca.* −48‰ in the shelf waters to −55‰ in the intermediate waters of the Arctic Ocean. Therefore, the water column contains significant fractions of bomb ^{14}C down to depths of *ca.* 1500–2000 m in all major basins (Figs. 4A–C, 6A, 8A). In the Eurasian Basin, traces of bomb ^{14}C can actually be found all the way to the bottom, as indicated by the presence of bomb ^{3}H (Figs. 5, 7, 9). The separation of the bomb ^{14}C signal from the natural ^{14}C signal in these waters is fairly difficult, and will not be attempted in the context of this contribution. We rather focus our effort on a purely descriptive treatment of the main features observed in the upper water column. However, for the deep waters, we present a semi-quantitative evaluation of the ^{14}C data below.

There is a pronounced $\Delta^{14}C$ gradient in the surface waters with a transition from low values in the southern Nansen Basin (≈ 50–70‰; Fig. 4A) to higher values in the northern Nansen Basin (≈ 80–120‰; Fig. 4C), the Amundsen Basin (≈ 100–120‰; Fig. 6A), and the Makarov Basin (≈ 120‰; Fig. 6A). The gradient reverses toward the southern Canada Basin, where surface $\Delta^{14}C$ values of only *ca.* 20–40‰ are observed (Fig. 8A).

The increase in surface $\Delta^{14}C$ in the Nansen, Amundsen and Makarov Basins is correlated with an increasing fraction of river runoff in the surface waters of those basins (see, *e.g.*, Schlosser *et al.* 1995; Bauch, Schlosser and Fairbanks 1995). The river runoff is also marked by high carbonate concentrations (see, *e.g.*, Anderson *et al.* 1989). A somewhat speculative interpretation of the high $\Delta^{14}C$ values in the river-runoff-tagged water is ^{14}C exchange of the surface and groundwaters feeding the Siberian Rivers with soil carbonates. Such a process would delay the input of ^{14}C from the bomb peak into the river runoff compared to open ocean surface waters, and would result in the observed high $\Delta^{14}C$ values in waters with high river runoff fractions.

$\Delta^{14}C$ values in the core of the Atlantic-derived water underlying the surface and halocline waters are fairly uniform (≈ 50‰) throughout the Arctic Ocean (Figs. 4, 6, 8). This feature seems to indicate that the bomb ^{14}C signal has been spread fairly homogeneously throughout this water layer during the past 25 yr, *i.e.*, the mean residence time of water in the Atlantic layer seems to be significantly faster than this time span.

Below the core of the Atlantic layer centered at *ca.* 300-m depth and the deep waters, $\Delta^{14}C$ values decrease monotonically in all basins to values of *ca.* −50‰ at depths of *ca.* 1500 m (central Nansen Basin) to *ca.* 2000 m in all other basins except the Makarov Basin, where the −50‰ isoline is at a much shallower depth of *ca.* 1000 m. This observation, together with the ^{3}H data, suggests that waters that have recently been in contact with the atmosphere penetrate less deeply in the Makarov Basin and the central Nansen Basin than in the other basins of the Arctic Ocean. The highest fraction of those recently ventilated waters at intermediate depth (1000–2000 m) is observed in the southern Canada Basin followed by the northern Nansen Basin and the Amundsen Basin. However, the ^{3}H data coverage of the Amundsen Basin is still very sparse, and firm conclusions have to wait until the $^{3}H/^{3}He$ data set has been completed. One might speculate that the recently ventilated intermediate waters correlated with a salinity maximum at *ca.* 600-m depth observed by Smethie *et al.* (1994) over the continental slope of the Laptev Sea are the source of the intermediate waters with relatively high $\Delta^{14}C$ and ^{3}H values found in the northern Nansen Basin, the Amundsen Basin and the southern Canada Basin. Such a scenario seems to be consistent with the circulation scheme that Rudels, Jones and Anderson (1994) proposed for the intermediate waters of the Arctic Ocean.

Deep Waters

Most of the deep waters of the Eurasian Basin contain a significant fraction of bomb ^3H ($\approx$ 0.05 TU in EBBW of the central Nansen Basin to $\approx$ 0.2–0.3 TU in EBBW of the Amundsen and Northern Nansen Basins; Figs. 5E, 5F, 7B). These waters then also contain a trace of bomb ^{14}C, preventing a straightforward conversion of their measured $\Delta^{14}C$ values into age information. However, $^3H/^{14}C$ correlations can be used to subtract the bomb ^{14}C from the observed $\Delta^{14}C$ values. The corrected $\Delta^{14}C$ values can then be converted into *isolation ages*. We define isolation age as the average time elapsed since the waters producing the deep waters have been isolated from exchange of ^{14}C with the atmosphere. The isolation age should not be confused with the *mean residence time* of a body of water. The mean residence time is a measure for the average time a water parcel spends in a certain reservoir of a deep basin, whereas the isolation age reflects the average time needed for surface waters to reach this deepwater reservoir. Consequently, the isolation age of a deep water reservoir can be significantly higher than its mean residence time.

Schlosser *et al.* (1995) have applied the above concept to the Nansen Basin. Here we summarize the main results of this study, which yielded isolation ages of *ca.* 150 yr for EBDW and *ca.* 250–300 yr for EBBW. These ages agree well with ^{39}Ar data and box model calculations tuned by transient and steady-state tracers (for details, see Schlosser *et al.* 1995; Bönisch and Schlosser 1995).

The deep waters of the Amundsen Basin have slightly higher $\Delta^{14}C$ values than those of the Nansen Basin ($\approx$ −72 to −75‰ compared to $\approx$ −75 to −83‰; Fig. 6B) which, if taken at face value, would translate into lower isolation ages. However, the higher ^3H concentrations of the deep waters in this basin require subtraction of a higher bomb ^{14}C component from the observed $\Delta^{14}C$ values. Using a $^3H/^{14}C$ correlation for the bottom waters of the Amundsen Basin extrapolated to a ^3H concentration of zero leads to a corrected $\Delta^{14}C$ value of *ca.* −85‰. This value is almost identical to that obtained for the bottom waters of the Nansen Basin, which means that the *old* component of EBBW in the Amundsen Basin, *i.e.*, the water free of surface water added during the past *ca.* 25 yr, has about the same isolation age as the EBBW in the central Nansen Basin. This is more-or-less free of bomb ^3H (Fig. 5E). The main difference between the two deep basins is the higher rate of addition of near-surface water tagged by transient tracers such as ^3H or bomb ^{14}C to the deep and bottom waters in the Amundsen Basin. This seems to result in slightly younger overall isolation ages (and mean residence times) of EBDW and EBBW in the Amundsen Basin compared to the Nansen Basin. This finding agrees well with the ^{39}Ar data. Quantification of this effect is beyond the scope of this contribution and will be done in combination with other tracer fields in a follow-up paper.

The deep waters of the Canadian Basin are practically ^3H-free at depths below *ca.* 2000 m (Makarov Basin) to 2500 m (southern Canada Basin; Fig. 9B). From this observation, we conclude that the contribution of bomb ^{14}C to these waters is negligible. Another remarkable feature of the ^{14}C distribution in the deep Canadian Basin is the homogeneous $\Delta^{14}C$ values. No detectable gradient in $\Delta^{14}C$ is present in the deep waters of the Makarov and southern Canada Basins, both vertically, at depths below 2000–2500 m, and laterally (Fig. 8B). The boundary below which the distribution of $\Delta^{14}C$ is extremely homogeneous coincides with the transition to a very weakly stratified water body (see σ_0 and σ_3 sections in Fig. 3). Assuming a mean $\Delta^{14}C$ value of −105‰ for the deep waters and a prebomb surface water $\Delta^{14}C$ value of −55‰ (Östlund, Possnert and Swift 1987), we calculate an isolation age for the deep waters of the Canadian basin of *ca.* 450 yr. ^{39}Ar data from the deep Makarov Basin (below 2500 m; Fig. 10) also suggest a higher isolation age compared to the Eurasian Basin. However, the straightforward estimate of the isolation age based on an ^{39}Ar concentration of *ca.* 40% yields only *ca.* 350 yr, a value significantly lower than that obtained from the ^{14}C data.

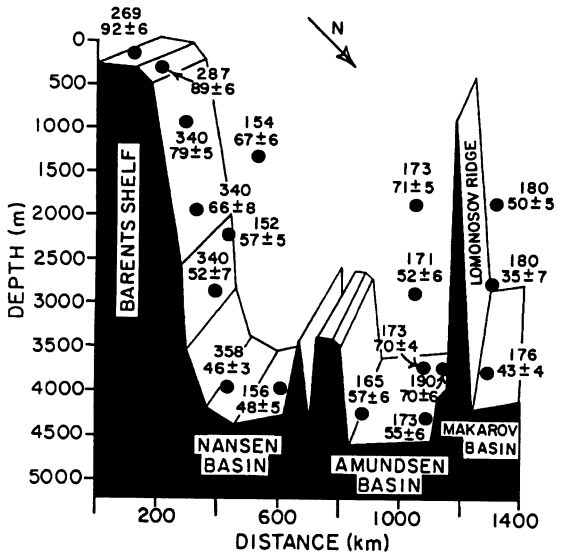

Fig. 10. ^{39}Ar concentrations observed in the Nansen, Amundsen, and Makarov basins of the Arctic Ocean. The numbers indicate the station number and the average ^{39}Ar concentration (in % modern; the uncertainty is the error of the mean value of up to three replicate measurements).

In light of the new data from the deepest waters in the Canada Basin, the age estimates of Östlund, Possnert and Swift (1987) were probably a few hundred years too high (they obtained mean isolation times of *ca.* 700–800 yr). Those measurements were made at an early stage of development of the AMS facility at Uppsala and, as stated by Östlund, Possnert and Swift (1987), had larger uncertainties than the radiometrically determined ^{14}C data reported in the same paper. Thus, the disagreement with the newer results in this contribution has a reasonable explanation.

^{14}C data have already been used to estimate the age of the deep water in the Canadian Basin. These estimates assumed different scenarios for the deepwater formation process. Inspired by the high ages of Canadian Basin deep waters derived by Östlund, Possnert and Swift (1987), Macdonald and Carmack (1991) and Macdonald, Carmack and Wallace (1992) assumed that the deep waters of the Canadian Basin are the remnant of a deepwater renewal event several hundred years ago. They further assume that the deepwater body formed in this way is now only eroded from the top by vertical turbulent exchange (eddy diffusion). Using the shape of the SJF $\Delta^{14}C$ profile (Fig. 8A), they calculated an exchange coefficient of $3.9 \times 10^{-5} m^2 sec^{-1}$ (Macdonald, Carmack and Wallace 1992). However, the few ^{14}C data points in the SJF profile probably misled these authors to believe that the deep $\Delta^{14}C$ profile has the shape of a quasi-exponential function consistent with a one-dimensional diffusion profile. New data points from a site close to the SJF station (PS 92; Jones *et al.* 1994) and from our Makarov Basin Station (176) clearly show no measurable $\Delta^{14}C$ gradient in the deep waters of the Canadian Basin. Therefore, the Macdonald and Carmack scenario does not seem to be consistent with the data. A turbulent exchange coefficient of $3.9 \times 10^{-5} m^2 sec^{-1}$ would lead to an erosion of the profile with a mean penetration depth of *ca.* 800 m. Such a feature is not consistent with the strictly constant $\Delta^{14}C$ profile below 2000 m in the Makarov Basin and below 2500 m in the southern Canada Basin (Fig. 8).

Jones *et al.* (1994) assumed a different scenario of a continuous renewal of the deep waters by shelf waters ($\Delta^{14}C$ value: –55‰) at a rate of *ca.* 0.01 Sv. They explain the vertical homogeneity of the $\Delta^{14}C$ profile below 2500 m as caused by a thick benthic boundary layer maintained by convection in a weakly stratified water body in analogy to the observations in the Black Sea by Murray, Top and Ozsoy (1991). Using this scenario, Jones *et al.* (1994) calculate an isolation age of the deep Canada Basin waters of 430 yr, a value practically identical with our estimate (≈ 450 yr) and that of Östlund, Possnert and Swift (1987) for the Makarov Basin (≈ 450 yr; this estimate was based on a single data point below 2000 m depth).

To estimate the mean residence time of CBDW, we apply a simple inverse model calculation based on the circulation scheme proposed by Jones, Rudels and Anderson (ms.). We assume that CBDW is

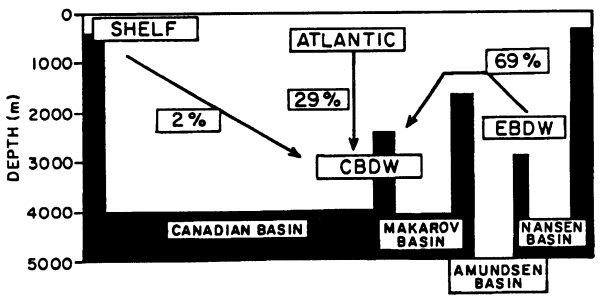

Fig. 11. Schematic view of the box model used to estimate the mean residence time of CBDW

a mixture of Atlantic Water, EBDW flowing over the Lomonosov Ridge into the deep Canadian Basin, and brine-enriched shelf water from the shelf seas surrounding the Canadian Basin. Assuming the salinities and potential temperatures listed in Table 1, we estimate the fractions of Atlantic Water, EBDW and Shelf Water to be *ca.* 29%, 69% and 2%, respectively (Fig. 11). Brine-enriched shelf water is typically low in $\delta^{18}O$ (*e.g.*, Bauch, Schlosser and Fairbanks 1995), and thus, cannot be a major contributor to the deep waters with $\delta^{18}O$ values close to those of Atlantic-derived water (*ca.* 0.3‰). However, the small fraction of shelf water derived from our simple inverse model approach is consistent with the observed $\delta^{18}O$ values in Arctic Ocean Deep Water (Bauch, Schlosser and Fairbanks 1995). After calculating the fractions of the individual water masses contributing to CBDW, we then use ^{14}C and ^{39}Ar data to estimate the mean residence time of CBDW under steady-state conditions. We obtain mean residence times of *ca.* 317 yr (^{14}C) and 293 yr (^{39}Ar), respectively. Within the errors of our estimates, these values are practically identical.

TABLE 1. Parameters used in the simple inverse box-model calculation of the fractions of Atlantic-derived water, EBDW and brine-enriched shelf water contained in CBDW, as well as the mean residence time of CDBW

Water mass	θ [°C]	Salinity	$\Delta^{14}C$ (‰)	^{39}Ar (% modern)
Shelf water	−1.8	36.5	−52	100
Atlantic-derived	0.8	34.9	−65	90
EBDW	−0.87	34.93	−74	66
CBDW	−0.4	34.95	−105	42

Although apparently more sensible than the scenario assuming the existence of a relict water body eroded by turbulent vertical exchange from the top, the continuous renewal hypothesis is not without problems. Continuous renewal at a rate of several per mil per year based on a mean renewal rate of *ca.* 300 yr results in a replacement of *ca.* 8% of deep water by near-surface water over a period of 25 yr, *i.e.*, the period during which bomb ^{3}H was present in these waters. Using the box model described by Bönisch and Schlosser (1995), we estimated the ^{3}H concentration of CBDW for steady-state conditions. The results indicate that CBDW collected during the 1980s should have ^{3}H concentrations close to the detection limit (≈ 0.05 TU; Fig. 12). However, the observed ^{3}H concentrations fall around *ca.* 0 TU, and might indicate discontinuous renewal from the surface. Therefore, we conclude that either deepwater formation in the Canadian Basin was discontinous (no deepwater formation during at least the past several decades), or that the newly formed deep water is confined to a boundary current from which it slowly mixes into the interior of the basin and has not yet reached Stations SJF and PS 92. Unfortunately, no ^{3}H data are available from Station PS 92, which is very close to the continental slope and should have detectable ^{3}H concentrations if the continuous renewal scenario is correct.

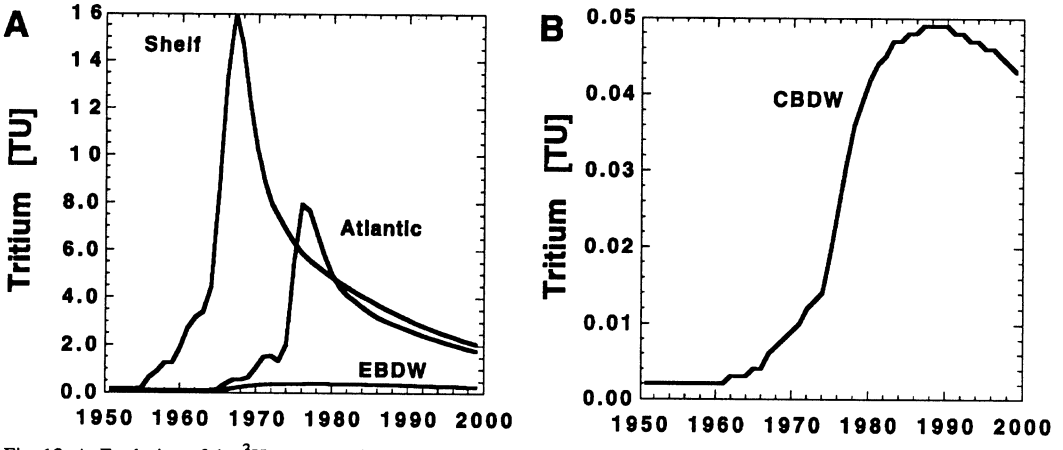

Fig. 12. A. Evolution of the ^{3}H concentration in Atlantic Water, EBDW and brine-enriched shelf water. B. Evolution of the ^{3}H concentration in CBDW (69% EBDW; 29% Atlantic Water; 2% brine-enriched shelf water) for steady-state conditions.

Conclusion

The data set presented above of all the major basins of the Arctic Ocean allows us to draw the following conclusions:

1. The deep and bottom waters of the Eurasian Basin (Nansen and Amundsen Basins) are significantly younger than those of the Canadian Basin (Makarov and Canada Basins). The mean isolation ages of the deep and bottom waters in the Eurasian Basin range from *ca.* 160 yr (≈ 1500–2600-m depth) to *ca.* 250–300 yr (bottom waters below 2600-m depth). These results are based on a pre-bomb surface $\Delta^{14}C$ value of −55‰ (Östlund, Possnert and Swift 1987) and are in agreement with box-model calculations tuned by transient tracers (^{3}H, CFC-11, CFC-12, ^{85}Kr). They further agree with estimates of the isolation age based on ^{39}Ar measurements (Schlosser *et al.* 1995).
2. The Lomonosov Ridge is an effective barrier for exchange of deep and bottom waters between the Eurasian and Canadian Basins of the Arctic Ocean. This results in significantly higher isolation ages of the deep and bottom waters in the Canadian Basin.
3. There is no measurable ^{14}C gradient between the deep waters of the Makarov Basin (depth ≥2000 m) and the southern Canada Basin (depth ≥2500 m). There is also no detectable vertical gradient in the deep waters of the Canadian Basin. A straightforward estimate of the isolation age of the deep Makarov and Canada Basins yields values of *ca.* 450 yr (pre-bomb surface $\Delta^{14}C$ value: −55‰). A straightforward estimate based on ^{39}Ar yields an isolation age of *ca.* 350 yr.
4. ^{3}H concentrations in the deep Canadian Basin are very close to or below the detection limit. If the renewal of deep water in the Canadian Basin were continuous, we would expect ^{3}H levels of ≈ 0.05 TU. From this observation, we conclude that the renewal of deep water in the Canadian Basin might be variable in time, and that it might have been reduced during the past few decades. Variability in deepwater formation has been observed in other parts of the coupled system Greenland-Norwegian Seas and Arctic Ocean (see, *e.g.*, Schlosser *et al.* 1991; Rhein 1991; Meincke, Jonsson and Swift 1992). An alternative explanation of our observations is renewal of deep water through narrow, confined boundary currents that have not yet been sampled for transient tracers. Input of CCl_4 to the oceans reaches further back in time. CCl_4 data from the Canadian Basin should therefore provide a better test of the hypotheses outlined above.

ACKNOWLEDGMENTS

This work profited from the contributions of numerous individuals and institutions. The Alfred-Wegener-Institut for Polar and Marine Research and the crew of RV *Polarstern* provided invaluable logistical assistance for the ARK IV and ARK VIII field programs. Andrea Ludin, Peter Marian, Matthias Meder and Jose Rodriguez helped to collect and degas the large volume ^{14}C samples at sea. The careful preparation of the ^{14}C sampling equipment by the workshop of the Institut für Umweltphysik under the leadership of Reiner Fletterer guaranteed two successful sampling campaigns. Jörn Thiede and Dieter Fütterer, chief scientists during ARK IV and ARK VIII, respectively, provided generous ship time for the collection of *ca.* 300 LV ^{14}C samples. Financial support was provided by the Office of Naval Research (Grant N00014-90-J-1362), the National Science Foundation (Grant DPP 90-22890) and the Deutsche Forschungsgemeinschaft. This is L-DEO contribution no. 5296.

REFERENCES

Aagaard, K., Coachman, L. K. and Carmack, E. C. 1981 On the halocline of the Arctic Ocean. *Deep-Sea Research* 28: 529–545.

Aagaard, K., Swift, J. H. and Carmack, E.C. 1985 Thermohaline circulation in the Arctic Mediterranean Seas. *Journal of Geophysical Research* 90: 4833–4846.

Anderson, L. G., Jones, E. P. Koltermann, K. P. Schlosser, P., Swift, J. H. and Wallace D. W. R. 1989 The first oceanographic section across the Nansen Basin in the Arctic Ocean. *Deep-Sea Research* 36: 475–482.

Bauch, D., Schlosser, P. and Fairbanks, R. 1995 Freshwater balance and sources of deep and bottom waters in the Arctic Ocean inferred from the distribution $H_2{}^{18}O$. *Progress in Oceanography,* in press.

Bönisch, G. and Schlosser, P. 1995 Deep water formation and exchange rates in the Greenland/Norwegian seas and the Eurasian Basin of the Arctic Ocean derived from tracer balances. *Progress in Oceanography,* in press.

Broecker, W. S., Gerard, R., Ewing, M. and Heezen, B. C. 1960 Natural radiocarbon in the Atlantic Ocean. *Journal of Geophysical Research* 65: 2903–2931.

Broecker, W. S., Peng, T.-H., Östlund, H. G. and Stuiver, M. 1985 The distribution of bomb radiocarbon in the ocean. *Journal of Geophysical Research* 90: 6953–6970.

Broecker, W. S., Blanton, S., Smethie, W. M. and Östlund, H. G. 1991 Radiocarbon decay and oxygen utilization in the deep Atlantic Ocean. *Global Biogeochemical Cycles* 5: 87–117.

Jones, E. P. and Anderson, L. G. 1986. On the origin of the chemical properties of the Arctic Ocean halocline. *Journal of Geophysical Research* 91: 10,759–10,767.

Jones, E. P., Rudels, B., and Anderson, L. G. (ms.) Deep waters in the Arctic Ocean: Origin and circulation. Submitted to *Deep-Sea Research.*

Jones, G. A., Gagnon, A. R., von Reden, K. F., McNichol, A. P. and Schneider, R. J. 1994 High-precision AMS radiocarbon measurements of central Arctic Ocean sea waters. *Nuclear Instruments and Methods in Physics Research,* in press.

Macdonald, R. W. and Carmack, E. C. 1991 Age of Canada Basin Deep Waters: A way to estimate primary production for the Arctic Ocean. *Science* 254: 1348–1350.

Macdonald, R. W., Carmack, E. C. and Wallace, D. W. R. 1992 ^{3}H and radiocarbon dating of Canada basin deep waters. *Science* 259: 103–104

Meincke, J., Jonsson, S. and Swift, J. H. 1992 Variability of convective conditions in the Greenland Sea. *ICES Marine Science Symposia* 195: 32–39

Münnich, K. O. and Roether, W. 1967 Transfer of bomb ^{14}C and ^{3}H from the atmosphere to the ocean; internal mixing of the ocean on the basis of tritium and ^{14}C profiles. In *Radioactive Dating and Methods of Low-Level Counting.* Vienna, IAEA: 93–103.

Murray, J. W., Top, Z. and Ozsoy, E. 1991 Hydrographic properties and ventilation of the Black Sea. *Deep-Sea Research* 38: S663–S689.

Östlund, H. G., Possnert, G. and Swift, J. H. 1987 Ventilation rate of the deep Arctic Ocean from carbon 14 data. *Journal of Geophysical Research* 92: 3769–3777.

Östlund, H. G., Top, Z. and Lee, V. E. 1982 Isotope dating of waters at Fram III. *Geophysical Research Letters* 9: 1117–1119.

Rhein, M. 1991. Ventilation rates of the Greenland and Norwegian Seas derived from distributions of the chlorofluoromethanes F11 and F12. *Deep-Sea Research* 38: 485–503.

Rudels, B., Jones, E. P. and Anderson, L. G. 1994 On the intermediate depth waters of the Arctic Ocean. *In* Johannessen, O. M., Muench, R. D. and Overland, J. E. *The Polar Oceans and their Role in Shaping the Global Environment.* AGU Geophysical Monograph 85. Washington, D.C., American Geophysical Union.

Schlosser, P., Bauch, D., Fairbanks, R. and Bönisch, G. 1994 Arctic river-runoff: Mean residence time on the shelves and in the halocline. *Deep-Sea Research* 41: 1053–1068.

Schlosser, P., Bönisch, G., Kromer, B., Loosli, H. H., Bühler, B., Bayer, R., Bonani, G. and Koltermann, K. P. 1995 Mid 1980s distribution of ^{3}H, ^{3}He, ^{14}C, and ^{39}Ar in the Greenland/Norwegian Seas and the Nansen Basin of the Arctic Ocean. *Progress in Oceanography*, in press.

Schlosser, P., Bönisch, G., Kromer, B., Münnich, K. O. and Koltermann, K. P. 1990 Ventilation rates of the waters in the Nansen Basin of the Arctic Ocean derived from a multi-tracer approach. *Journal of Geophysical Research* 95: 3265–3272.

Schlosser, P., Bönisch, G., Rhein, M., and Bayer, R. 1991 Reduction of deepwater formation in the Greenland Sea during the 1980s: Evidence from tracer data. *Science* 251: 1054–1056.

Smethie, W. M., Jr., Chipman, D. W., Swift, J. H. and Koltermann, K. P. 1988 Chlorofluoromethanes in the Arctic Mediterranean seas: Evidence for formation of bottom water in the Eurasian Basin and deep water exchange through Fram Strait. *Deep-Sea Research* 35: 347–369.

Smethie, W. M., Jr., Frank, M., Muench, R., Bayer, R. and Schauer, U. 1994 Tracer and hydrographic observations along the continental slopes of the Barents and Laptev seas. *EOS* 75: 117.

Stuiver, M., Quay, P. and Östlund, H. G. 1983 Abyssal water carbon-14 distribution and the age of the world's oceans. *Science* 219: 849–851.